International Journal of Engineering

A Novel Sensor Integration Scheme for an Aided Inertial Navigation System Based on a Generalized PID Filter in the Presence of Observation Uncertainty

M. Ansari[a], J. Jamali[*a], M. H. Fatehi-Dindarlou[a], M. A. Rahgoshay[b], O. Mahdiyar[a]

[a] Islamic Azad University of Kazerun, Department of Electrical Engineering, Kazerun, Iran
[b] Salman Farsi University of Kazerun, Department of Electrical Engineering, Kazerun, Iran

P A P E R   I N F O

A B S T R A C T

Implementing a proper integration scheme plays an important role in the performance of integrated navigation systems. Not only does employing a more reliable estimation method improve the accuracy of the integrated navigation system, but this can lead to a more robust solution in the presence of different types of uncertainties. Implementing an integration scheme that has a robust and simple structure is a challenging issue in the design of integrated navigation systems. By inspiring from the concept of PID control, this paper proposes a robust integration scheme for aided inertial navigation systems in the presence of aiding sensor measurement uncertainties. The proposed filter combines the concept of proportional-integral-derivative control theory and the standard Kalman filter estimator to improve the performance of the integration scheme. Thanks to the integral and derivative parts added to the proposed scheme, the integrated system attains a faster and more robust solution in the presence of observation errors and uncertainties. The simulation case studies validate the superior efficacy and capability of the proposed scheme compared to the integration method based on the standard Kalman filter.

Graphical Abstract

Standard INS/GPS Integrated System   GPID INS/GPS Integrated System
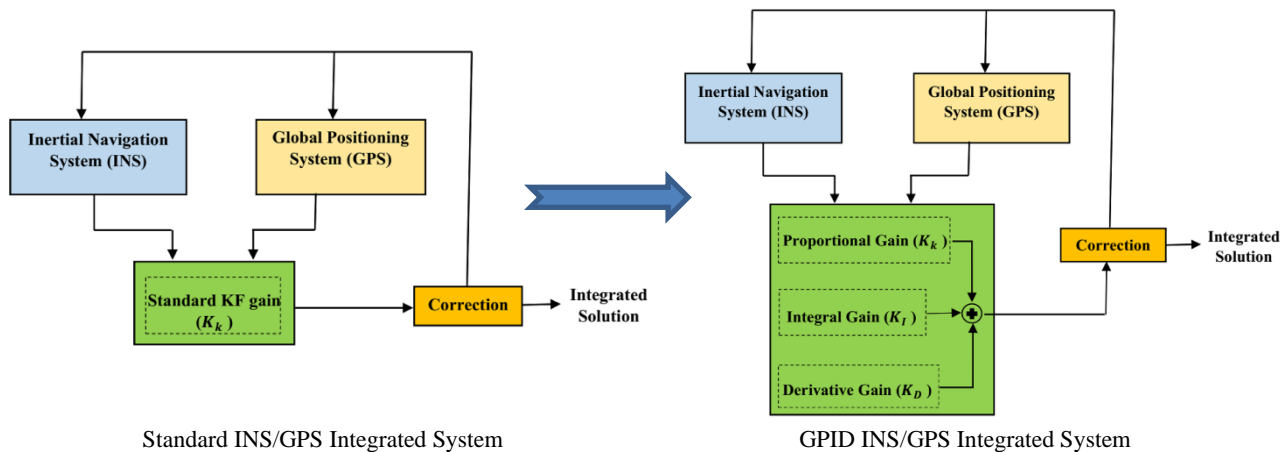
1. INTRODUCTION

Navigation systems can function based on two different techniques: Dead Reckoning (DR) and Position Fixing

(PF) (1) . DR-based systems utilize the measurements of the vehicle's motions via body-mounted inertial sensors and perform a series of computational tasks to obtain the navigation solution. On the other hand, PF-based systems

*Corresponding Author Email: j.jamali@kau.ac.ir (J. Jamali)

attain the navigation solution by exchanging data with the known position information of external sources. The solution obtained by the DR-based system usually has an appropriate performance in short-term intervals but the accumulative error caused by the integration operation deteriorates the accuracy and performance of the long-term solution. Unlike DR-based systems, PF-based systems represent a desirable long-term but noisy short-term solution. To benefit from the advantages and cover the drawbacks of the two aforementioned techniques, aided or integrated navigation systems utilize both DR and PF systems simultaneously, which leads to a more precise and reliable navigation solution (2). As the most well-known DR-based navigation system, the Inertial Navigation System (INS) usually uses external information of one or more PF-based systems as aiding sensors. For instance, INS-aided systems such as INS/Global Navigation Satellite System (GNSS) and INS/Doppler Velocity Log (DVL) are widely used in land, aerial and marine (3-5).

One of the most important parts of an integrated navigation system is the optimal state estimator, which continuously estimates the navigation system's errors during the initial alignment and navigation stages. The performance of an aided navigation system is directly affected by optimal state estimation techniques used in the integration or sensor fusion scheme. Kalman Filter (KF) is the most widely used optimal state estimator in many theorical and industrial applications including integrated navigation systems (6-11). To achieve an optimal solution in the KF, determining proper models for the system and stochastic noises is a key factor problem (12). In the integrated navigation system, the system model is mostly deterministic and does not raise a serious issue in the KF-based estimator. However, determining a proper stochastic model for process and measurement noises (Q and R) is a challenging issue. In fact the statistical model of inertial sensors, gyroscopes and accelerometers, is specified by an error covariance matrix, Q. Also, the measurement error of aided sensors which are utilized in the aided navigation system is specified by another error covariance matrix, R.

A proper model for Q is usually obtained according to the specification of inertial sensors and nominal dynamic motion which vehicle experiences. However, the modeling of R is not as straightforward as Q. In fact, the outputs of the PF-based system used as the measurement vector in the estimator can be corrupted by several sources of errors, which possibly decreases the performance of the integrated system. The GPS measurement, for instance, may suffer from different types of errors such as multipath, interference or jamming, receiver and satellite clock offsets, etc. Similarly, the velocity measurements of a DVL can also be associated with errors such as bias and noise due to installation misalignment, severe environmental

conditions, temporary failures, etc. Clearly, setting a fixed R model for the optimal estimator may not be a viable option and does not attain an optimal solution for the integrated system.

2. RELATED WORK

In recent research, robust and adaptive solutions are proposed to resolve the lack of robustness issue in the KF estimator of the integrated navigation systems (13-15). However, these methods assume predetermined constraints on the signal uncertainty model and also add some complexity to the signal processing algorithms of the estimation procedure.

The concept of a combination of the PID control theory and the standard KF has recently been presented in some research (16-18). This idea leads to a simple structure and robust estimator named the Generalized Proportional Integral Derivative (GPID) filter. In addition to current measurement, the GPID filter also uses past and prediction of future measurements to estimate the current state and attains a more desirable performance compared to the standard KF. The GPID filter was used in the initial self-alignment of SINS for the first time (19, 20). The self-alignment process is performed by stationary or quasi-stationary assumptions without using any external aided measurements. This process usually utilizes measures of the Earth's rotation rate and the gravity vector in different frames as the measurement vector which are pure and do not have any uncertainties in them. Therefore, Q modeling is much more important than R modeling in the initial self-alignment process. On the other hand, in the integrated navigation systems, unlike the initial self-alignment process, R modeling plays a critical role in the integrated system due to the existence of uncertainties in the observations (measurements) of aiding sensors. In the presence of these uncertainties, improper R modeling can greatly decrease the performance of the integrated system.

In this paper, a robust integration scheme for the INS-aided system is proposed based on the GPID filter as the optimal estimator. Regarding the robustness property of the proposed approach, the performance of the integrated system is greatly improved in the presence of observation uncertainties compared with the standard KF-based integration scheme. The proposed scheme also has a simple structure and low computational burden compared to the robust and adaptive KF-based schemes. By conducting simulation case study tests, the efficacy and capability of the proposed method are demonstrated and compared with the standard KF-based integration scheme.

The contributions of the paper are as follows:

- Proposing a novel PID-based Kalman filter for the integrated navigation systems
- Proposing a simplified structure of GPID Filter for simple online implementation
- Presenting a detailed robustness analysis of the proposed integration scheme

The paper is divided into the following sections. In section 2, the process and measurement equations used in the integration scheme are introduced. The main contribution of the proposed method is expressed in section 3, which contains the introduction of the GPID filter for the integration scheme and also presents proof of the robustness of the proposed filter in the presence of the measurement uncertainty of the aiding sensor. Finally, in section 4, the proposed method has been evaluated through conducting a detailed simulation case study (section 5). The last part, this work is concluded in section 6.

3. THE ERROR DYNAMICS AND MEASUREMENT MODELS OF THE AIDED-INS

In this paper, a 9-state error dynamics model of Strapdown INS (SINS) is implemented. For most terrestrial applications, the simplified 9-state model is used without causing a considerable error. This model can be expressed as follows:

$$\dot{\mathbf{x}}(t) = \mathbf{F}\mathbf{x}(t) + \mathbf{G}\mathbf{w}_p(t) \tag{1}$$

Where

$$\mathbf{x} = [\delta\boldsymbol{\varphi}^n_{3\times1} \quad \delta\mathbf{v}^n_{3\times1} \quad \delta\mathbf{p}^n_{3\times1}]^T \tag{2}$$

denotes the state vector with

$$\delta\boldsymbol{\varphi}^n = [\delta\varphi_E \; \delta\varphi_N \; \delta\varphi_U]^T \tag{3}$$

$$\delta\mathbf{v}^n = [\delta v_E \; \delta v_N \; \delta v_U]^T \tag{4}$$

$$\delta\mathbf{p}^n = [\delta L \; \delta l \; \delta h]^T \tag{5}$$

Equations 3 to 5 represents the attitude, velocity and position error vectors in the ENU local-level frame, respectively.

The process noise vector expressed as

$$\mathbf{w}_p = [\delta\omega^n \quad \delta a^n]^T \tag{6}$$

where Equations 7 and 8 denote the projection of the stochastic parts of gyroscopes and accelerometers measurement into the ENU-frame, respectively.

$$\delta\omega^n = [\delta\omega_E \; \delta\omega_N \; \delta\omega_U]^T \tag{7}$$

$$\delta a^n = [\delta a_E \; \delta a_N \; \delta a_U]^T \tag{8}$$

and The matrices $\mathbf{F}$ and $\mathbf{G}$ are also as follows:

$$\mathbf{F} = \begin{bmatrix} \mathbf{0}_{3\times3} & \mathbf{F}_{\varphi v} & \mathbf{0}_{3\times3} \\ \mathbf{F}_{v\varphi} & \mathbf{0}_{3\times3} & \mathbf{0}_{3\times3} \\ \mathbf{0}_{3\times3} & \mathbf{F}_{pv} & \mathbf{0}_{3\times3} \end{bmatrix} \tag{9}$$

$$\mathbf{G} = \begin{bmatrix} -\mathbf{I}_{3\times3} & \mathbf{0}_{3\times3} \\ \mathbf{0}_{3\times3} & \mathbf{I}_{3\times3} \\ \mathbf{0}_{3\times3} & \mathbf{0}_{3\times3} \end{bmatrix} \tag{10}$$

where,

$$\mathbf{F}_{\varphi v} = \begin{bmatrix} 0 & \frac{1}{(R_M+h)} & 0 \\ -\frac{1}{(R_N+h)} & 0 & 0 \\ -\frac{tanL}{(R_N+h)} & 0 & 0 \end{bmatrix} \tag{11}$$

$$\mathbf{F}_{v\varphi} = \begin{bmatrix} 0 & f_U & -f_N \\ -f_U & 0 & f_E \\ f_N & -f_E & 0 \end{bmatrix} \tag{12}$$

$$\mathbf{F}_{pv} = \begin{bmatrix} 0 & \frac{1}{(R_M+h)} & 0 \\ \frac{1}{(R_N+h)cosL} & 0 & 0 \\ 0 & 0 & 1 \end{bmatrix} \tag{13}$$

In the INS/GPS integrated system, the estimator takes the difference between INS and GPS velocity and position outputs as the measurement vector. The measurement model used in the estimator can be expressed as the following equations:

$$\mathbf{z}(t) = \begin{bmatrix} \mathbf{v}_{INS} - \mathbf{v}_{GPS} \\ \mathbf{p}_{INS} - \mathbf{p}_{GPS} \end{bmatrix} = \mathbf{C}\mathbf{x}(t) + \mathbf{w}_m(t) \tag{14}$$

where

$$\mathbf{C} = \begin{bmatrix} \mathbf{0}_{3\times3} & \mathbf{I}_{3\times3} & \mathbf{0}_{3\times3} \\ \mathbf{0}_{3\times3} & \mathbf{0}_{3\times3} & \mathbf{I}_{3\times3} \end{bmatrix} \tag{15}$$

and $\mathbf{w}_m$ is the measurement noise vector.

Similar to many other applications, the discrete form of the space-state model is commonly used in the estimation procedure of INS/GPS integration. The discrete-time form of Equations 1 and 14 are expressed as follows:

$$\mathbf{x}(k + 1) = \mathbf{A}\mathbf{x}(k) + \mathbf{w}_p(k) \tag{16}$$

$$\mathbf{y}(k) = \mathbf{H}\mathbf{x}(k) + \mathbf{w}_m(k) \tag{17}$$

where $\mathbf{x}(k)$ and $\mathbf{y}(k)$ are the state and measurement vectors. $\mathbf{A}$ and $\mathbf{H}$ are the discrete representations of matrices $\mathbf{F}$ and $\mathbf{C}$, respectively. $\mathbf{w}_p$ and $\mathbf{w}_m$ are assumed as a zero-mean stochastic vector with the covariance matrices of Q and R, respectively.

4. THE PROPOSED INTEGRATION SCHEME BASED ON GENERALIZED PID FILTER

In references, the standard KF is utilizzed as the estimator part of the integrated navigation systems. The block diagram of the INS/GPS integration based on the standard KF is depicted in Figure 1. According to this block diagram, the INS's computed velocity and position are compared with the GPS velocity and position
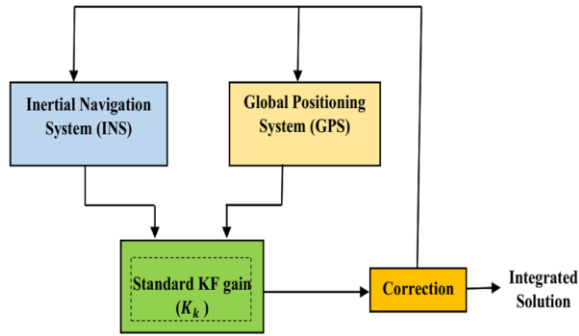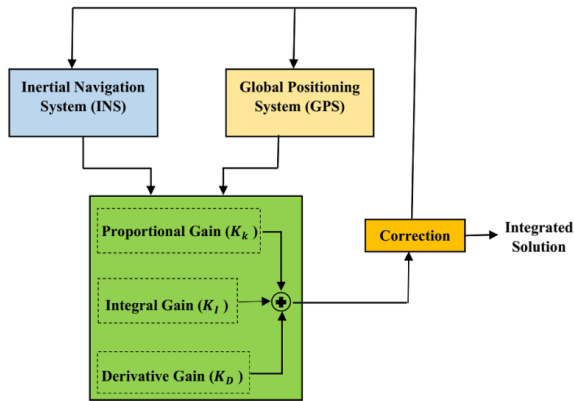
Figure 1. The block diagram of the INS/GPS integration based on the Standard KF

measurements, which are considered as the measurement vector in the KF estimator. At each cycle, the KF estimator computes an optimal Kalman gain K_k and estimates the errors related to INS and GPS. Finally, the estimated errors are feedback to INS and GPS systems and the integrated solution is attained.

As stated previously, the standard KF estimator is highly dependent on process and measurement models, which is the primary reason that motivated us to propose a robust integration scheme based on the combination of the PID control theory and the KF estimator. The block diagram of the proposed integration scheme is illustrated in Figure 2. Unlike the standard KF-based integration scheme, the proposed scheme utilizes two additional parts (integral and derivative parts) in its estimator block. The proposed scheme is the general form of the standard KF-based integration scheme and when the integral and derivative gains are set to zero, the GPID filter is identical to the standard KF.

Based on the error dynamics and measurement models of the INS/GPS integration described in Equations 1 to 17, the equations of the GPID estimator can be written as follows:

Figure 2. The block diagram of the INS/GPS integration based on the generalized PID filter

$$\hat{\mathbf{x}}(0|0) = \bar{\mathbf{x}}_0 \tag{18}$$

$$\mathbf{x}_I(0) = \mathbf{0} \tag{19}$$

$$\tilde{\mathbf{y}}(0) - \tilde{\mathbf{y}}(-1) = \mathbf{0} \tag{20}$$

$$\tilde{\mathbf{y}}(k) = \mathbf{y}(k) - \mathbf{H}\hat{\mathbf{x}}(k|k) \tag{21}$$

$$\hat{\mathbf{x}}(k|k-1) = \mathbf{A}\hat{\mathbf{x}}(k-1|k-1) \tag{22}$$

$$\mathbf{r}(k) = \mathbf{y}(k) - \mathbf{H}\hat{\mathbf{x}}(k|k-1) \tag{23}$$

$$\mathbf{x}_P(k) = \mathbf{K}_P(k)\mathbf{r}(k) \tag{24}$$

$$\mathbf{x}_I(k) = \mathbf{x}_I(k-1) + \mathbf{K}_I(k)\tilde{\mathbf{y}}(k-1) \tag{25}$$

$$\mathbf{x}_D(k) = \mathbf{K}_D(k)\big(\tilde{\mathbf{y}}(k-1) - \tilde{\mathbf{y}}(k-2)\big) \tag{26}$$

$$\hat{\mathbf{x}}(k|k) = \hat{\mathbf{x}}(k|k-1) + \mathbf{x}_P(k) + \mathbf{x}_I(k) + \mathbf{x}_D(k) \tag{27}$$

where $\mathbf{K}_P$, $\mathbf{K}_I$ and $\mathbf{K}_D$ denotes the proportional, integral and derivative gains used in computation of the proportional, integral and derivative parts of the estimator $\mathbf{x}_P$, $\mathbf{x}_I$ and $\mathbf{x}_D$, respectively.

Based on Equation 18 to 27, we have proposed a simple structured PID filter which has a desirable robustness property and low computational burden for online implementation. The equations of the SRPIF are as follows:

$$\mathbf{P}(0|0) = \mathbf{P}_0 \tag{28}$$

$$\mathbf{P}(k|k-1) = \mathbf{A}\,\mathbf{P}(k-1|k-1)\,\mathbf{A}^T + \mathbf{W}(k-1) \tag{29}$$

$$\mathbf{K}_P(k) = \mathbf{P}(k|k-1)\,\mathbf{H}^T\,(\mathbf{H}\,\mathbf{P}(k|k-1)\,\mathbf{H}^T + \mathbf{R}(k)\,)^{-1} \tag{30}$$

$$\mathbf{K}_I(k) = \mathbf{k_i} * \mathbf{K}_P(k) \tag{31}$$

$$\mathbf{K}_D(k) = \mathbf{k_d} * \mathbf{K}_P(k) \tag{32}$$

$$\mathbf{P}(k|k) = (\mathbf{I} - \mathbf{K}_P(k)\mathbf{C})\mathbf{P}(k|k-1) \tag{33}$$

$$\hat{\mathbf{x}}(k|k) = \hat{\mathbf{x}}(k|k-1) + \mathbf{x}_P(k) + \mathbf{x}_I(k) + \mathbf{x}_D(k) \tag{34}$$

where $\mathbf{k_i}$ and $\mathbf{k_d}$ are the integral and derivative constants and $\mathbf{x}_P$, $\mathbf{x}_I$ and $\mathbf{x}_D$ are determined by Equations 24 to 26, respectively.

4. 1. Robustness Analysis of the Proposed GPID Integration Scheme   Regarding the integral part employed in the generalized PID filter, the proposed integration scheme presents a robust solution, which successfully mitigates the undesirable effect of GPS signal uncertainties and errors on the integrated navigation system. To illustrate the effectiveness of the proposed scheme, the following robustness analysis is

presented based on the SRPIF estimator with $k_i=1$ and $k_d=0$. Because the GPS measurement uncertainties have a major effect on the performance of INS/GPS integration, the measurement noise is only considered in this analysis.

As mentioned before in the introduction, the main challenge in an integrated navigation system is detecting or eliminating the effect of aiding sensor measurement errors on the system performance. The specification of process noise is only related to inertial sensors used in the INS process and can be predetermined by some experimental laboratory tests. Therefore, the GPID integration scheme is proposed to eliminate the measurement error vector in aided INS. Hence, without loss of generality, we consider the state-space Equations 16 to 17 without the process noise vector :

$$\mathbf{x}(k + 1) = \mathbf{A}\mathbf{x}(k) \tag{35}$$

$$\mathbf{y}(k) = \mathbf{H}\mathbf{x}(k) + \mathbf{w}_m(k) \tag{36}$$

Based on the Equations 23 to 36, the one-step estimator can be written as follows:

$$\hat{\mathbf{x}}(k + 1|k + 1) = \mathbf{A}\hat{\mathbf{x}}(k|k) + \mathbf{K}_P\big(\mathbf{y}(k) - \mathbf{H}\hat{\mathbf{x}}(k|k)\big) + \mathbf{x}_I(k) \tag{37}$$

The estimation error is also defined as:

$$\mathbf{e}(k + 1) = \mathbf{x}(k + 1) - \hat{\mathbf{x}}(k + 1|k + 1) \tag{38}$$

Substituting Equations 25 to 37 into Equation 38 gives:

$$\mathbf{e}(k + 1) = \mathbf{A}\mathbf{x}(k) - \mathbf{A}\hat{\mathbf{x}}(k|k) - \mathbf{K}_P\mathbf{H}\mathbf{x}(k) + \mathbf{K}_P\mathbf{H}\hat{\mathbf{x}}(k|k) - \mathbf{K}_P\mathbf{w}_m(k) - \mathbf{x}_I(k) = (\mathbf{A} - \mathbf{K}_P\mathbf{H})\mathbf{e}(k) - \mathbf{K}_P\mathbf{w}_m(k) - \mathbf{x}_I(k) \tag{39}$$

The disturbance vector $\mathbf{d}(k)$ is defined as:

$$\mathbf{d}(k) = -\mathbf{K}_P\mathbf{w}_m(k) - \mathbf{x}_I(k) \tag{40}$$

Therefore, the error dynamics equation becomes:

$$\mathbf{e}(k + 1) = (\mathbf{A} - \mathbf{K}_P\mathbf{H})\mathbf{e}(k) + \mathbf{d}(k) \tag{41}$$

The dynamic equation of $\mathbf{d}(k)$ can be also written using Equations 21 and 25:

$$\mathbf{d}(k + 1) = -\mathbf{K}_P\mathbf{w}_m(k + 1) - \mathbf{x}_I(k + 1) = -\mathbf{K}_P\mathbf{w}_m(k + 1) - \mathbf{x}_I(k) - \mathbf{K}_I\mathbf{C}\mathbf{e}(k) \tag{42}$$

Adding and subtracting $-\mathbf{K}_P\mathbf{w}_m(k)$ to Equation 42 gives:

$$\mathbf{d}(k + 1) = \mathbf{d}(k) - \mathbf{K}_P\big(\mathbf{w}_m(k + 1) - \mathbf{w}_m(k)\big) - \mathbf{K}_I\mathbf{C}\mathbf{e}(k) \tag{43}$$

According to Equations 41 and 43 the augmented error dynamics can be expressed as:

$$\begin{bmatrix} \mathbf{e}(k + 1) \\ \mathbf{d}(k + 1) \end{bmatrix} = \begin{bmatrix} (\mathbf{A} - \mathbf{K}_P\mathbf{C}) & \mathbf{I}_{9\times9} \\ -\mathbf{K}_I\mathbf{C} & \mathbf{I}_{9\times9} \end{bmatrix} \begin{bmatrix} \mathbf{e}(k) \\ \mathbf{d}(k) \end{bmatrix} + \begin{bmatrix} \mathbf{0}_{9\times9} \\ -\mathbf{K}_P\big(\mathbf{w}_m(k + 1) - \mathbf{w}_m(k)\big) \end{bmatrix} \tag{44}$$

In INS, gyroscopes and accelerometer intrinsically attain their output measurements with a high rate (100Hz or higher) compared to low-rate updates of aiding sensors (21). Based on this realistic idea, there is a negligible difference between two consecutive outputs of the inertial sensors. Therefore, Equation 44 can be approximated as:

$$\begin{bmatrix} \mathbf{e}(k + 1) \\ \mathbf{d}(k + 1) \end{bmatrix} \approx \begin{bmatrix} (\mathbf{A} - \mathbf{K}_P\mathbf{C}) & \mathbf{I}_{9\times9} \\ -\mathbf{K}_I\mathbf{C} & \mathbf{I}_{9\times9} \end{bmatrix} \begin{bmatrix} \mathbf{e}(k) \\ \mathbf{d}(k) \end{bmatrix} \tag{45}$$

According to Equation 45, if the $\mathbf{K}_P$ and $\mathbf{K}_I$ are chosen appropriately, $\begin{bmatrix} (\mathbf{A} - \mathbf{K}_P\mathbf{C}) & \mathbf{I}_{9\times9} \\ -\mathbf{K}_I\mathbf{C} & \mathbf{I}_{9\times9} \end{bmatrix}$ becomes a stable matrix and the augmented error dynamics vector tends to zero as $k \rightarrow \infty$. Tending $\mathbf{d}(k)$ to zero means that the integral part of estimator, $\mathbf{x}_I(\mathrm{k})$, eliminates the undesirable effect of vector $-\mathbf{K}_P\mathbf{w}_m(k)$ ∎

5. SIMULATION CASE STUDY

To evaluate the performance of the proposed integration scheme, a comprehensive simulation case study is conducted in this section. In addition to the lack of access to a real experimental integrated navigation system, we conducted the simulation test to easily manipulate the GPS measurement and produce artificial errors in the GPS measurements in specific intervals. This paper uses the mathematical model and MATLAB simulation expressed by Zhang et al. (22) to generate the IMU and GPS measurements, which developed four different kinds of scenarios named static, straight line, circle, and s-shape trajectories. The specifications of the IMU and GPS errors added to the generated ideal measurements are shown in Table 1.

Inertial navigation systems are divided into different grades based on their accuracy and performance, which is directly related to the error specifications of inertial sensors implemented in the navigation system. In this paper, we assume that a tactical grade INS is used in the test with error specification in Table 1. However, choosing different grades of INS directly affects the performance of the integrated system, we implemented the same error specification in Table 1 to specifically evaluate the effect of the integration scheme on the performance of the aided navigation system. After

TABLE 1. Specification of the IMU and GPS errors

Gyro constant errors	0.01 deg / h
Gyro random errors	0.001 deg / $\sqrt{h}$
Accelerometer constant errors	±50 μg
Accelerometer random errors	0.03 $m/s/\sqrt{h}$
GPS receiver position error	5 m
GPS receiver velocity error	0.1 m/s

generating the IMU and GPS measurements, the integration schemes based on the standard KF and the proposed generalized PID filter are evaluated separately.

As we mentioned before, multipath error is the major source of GPS signal error that can happen in urban areas near tall buildings or dense jungles. To evaluate the performance of the proposed scheme, the GPS measurement is deliberately corrupted by multipath error in a specific time interval of the simulation test. The circle scenario is chosen for the motion trajectory of the INS/GPS integrated system. The total simulation time is considered as 1 hour (3600 seconds). It is assumed that the GPS signal is corrupted by some sources of multipath error in the interval of 600 to 1100 seconds. In this interval, the GPS position and velocity measurements are manipulated by multipath errors specified in Table 2.

In the simulation tests two different tunings of integral and derivative parts are used in the proposed integration:

scheme 1. ($k_i = 1$ & $k_d = 0$)
scheme 2. ($k_i = 1.5$ & $k_d = 3$).

However, other different options for these constants are viable and can be tested and utilized in the system, we choose these two different schemes to optimally illustrate the effect of integral and derivative parts with an acceptable response for the INS/GPS system.

The simulation test results for attitude errors are depicted in Figures 3 to 5. From these results and computed RMS attitude errors given in Table 3. It is clear that the standard KF estimator has an inaccurate solution in the presence of the GPS position and velocity error especially in the yaw angle, which converges more slowly after the error interval. However, the proposed method maintains the attitude errors near zero in the interval that the multipath error occurs. It can be concluded from the results that the proposed method can also be used in inertial gyrocompass systems where guaranteeing accurate angular positions is a critical issue, especially in marine applications.

TABLE 2. Specification of the IMU and GPS errors

|	
GPS position error corrupted by multipath	50 m
GPS receiver velocity error corrupted by multipath	0.5 m/s

TABLE 3. Attitude errors for the standard KF and proposed PID KF integration schemes

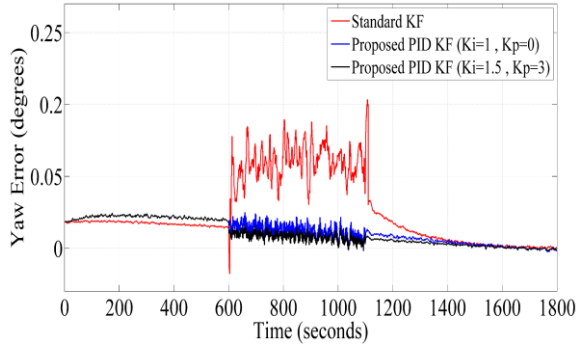| Integration method	Roll RMS Error (degree)	Pitch RMS Error (degree)	Yaw RMS Error (degree)
Standard KF	0.0665	0.0683	0.1538
Proposed PID KF (scheme 1)	0.0176	0.0188	0.0441
Proposed PID KF (scheme 2)	0.0159	0.0169	0.0402

The simulation results for latitude, longitude and altitude errors are depicted in Figures 6 to 8, respectively. The total path trajectory in the 2-D plane of longitude-latitude is also depicted individually in Figure 9 for both the standard KF and the proposed method with respect to the ideal trajectory. A detailed position error comparison is also given in Table 4 for both integration schemes. The results indicate that the positioning results of the proposed method have a more accurate and robust solution in response to the GPS multipath error. Based on the PID control theory, increasing the derivative constant, k_d, can result in the improvement of rapidness but also increase the oscillations in the response. On the other hand, the integral constant directly influences the accuracy of the response. The higher the integral constant k_I, the less error can be obtained in the response. Different tunings of the integral and derivative constants directly affect the performance of the proposed filter, which is reflected in the oscillation, rapidness, and accuracy of the solution. By a proper tunning of the integral and derivative constants, an acceptable filter performance can be achieved for a specific aided inertial navigation system. As is clear from the results, the proposed GPID filter of scheme 2 has a more accurate but more oscillatory response compared to the proposed GPID of scheme 1.
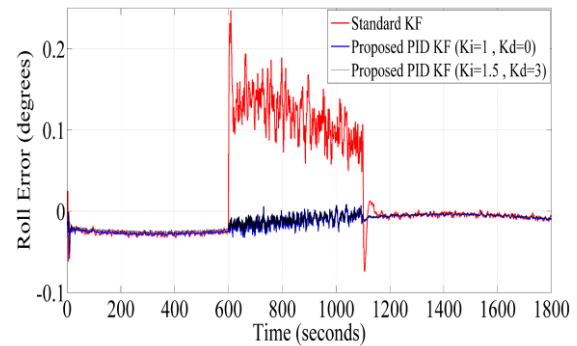
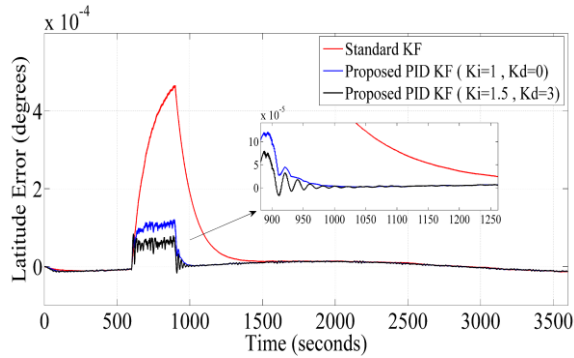**Figure 3.** Roll angle error of the standard KF and the proposed GPID filter schemes
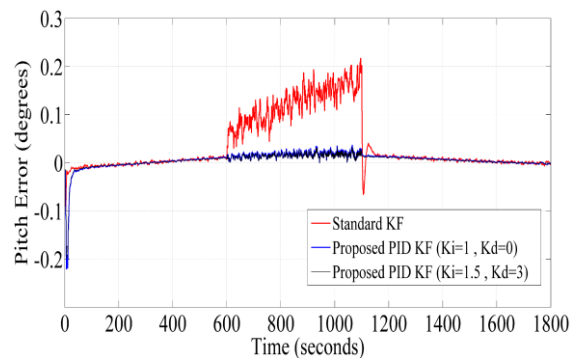
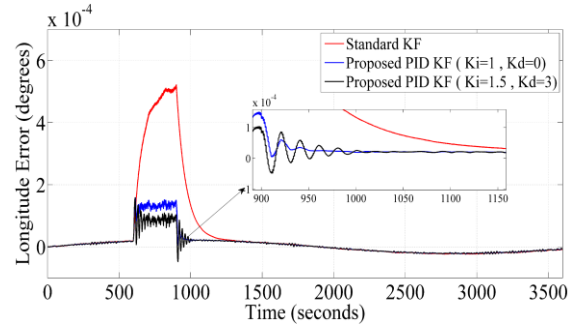**Figure 4.** Pitch angle error of the standard KF and the proposed GPID filter schemes

Figure 5. Yaw angle error of the standard KF and the proposed GPID filter schemes

TABLE 4. Position errors for the standard KF and proposed PID KF integration methods

| Integration method	Latitude RMS Error (degree)	Longitude RMS Error (degree)	Altitude RMS Error (meter)	Horizontal Position Error (Km)
Standard KF	10.6 e-05	18.8 e-05	61.39	1.37
Proposed PID KF (scheme 1)	4.25 e-05	5.58 e-05	16.49	0.44
Proposed PID KF (scheme 2)	2.61 e-05	3.95 e-05	11.04	0.30

Figure 6. Latitude error of the standard KF and the proposed GPID filter schemes

Figure 7. Longitude error of the standard KF and the proposed GPID filter schemes
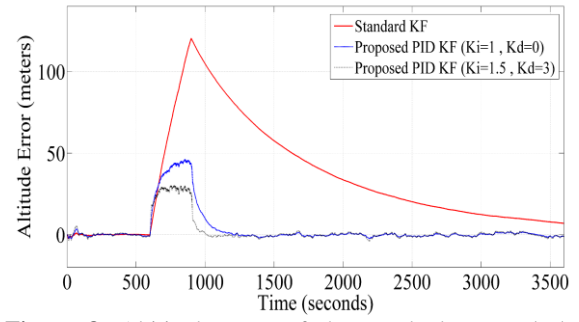
Figure 8. Altititude error of the standard KF and the proposed GPID filter schemes
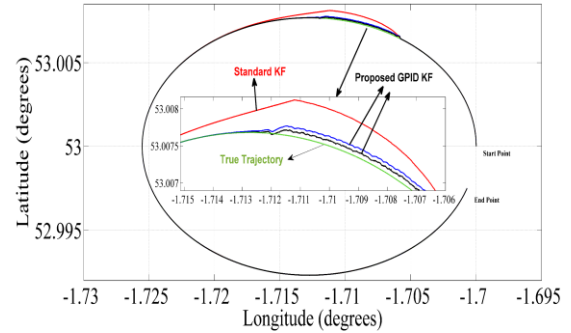
Figure 9. The 2-D trajectory for the KF and proposed GPID filter schemes

6. CONCLUSION

The performance of conventional estimators based on the standard Kalman filter is highly dependent on the accuracy of system and sensor modeling, which leads to performance reduction in the solution of the integrated navigation systems when the aiding sensor's information is corrupted by different sources of errors. To solve this problem, this paper has presented a robust simple structure integration scheme based on the combination of the PID control theory with the Kalman filter estimator. Adding two additional integral and derivative parts to the standard KF integration scheme can significantly boost the performance of the integrated navigation system. The proposed integration scheme is capable of eliminating the adverse effects of the measurement error of the aiding sensor in comparison to the standard KF scheme. The simulation results have illustrated that the proposed method has an acceptable performance in the presence of GPS measurement uncertainties in an INS/GPS navigation system. While The proposed integration scheme attains a robust solution with a very simple structure, which is suitable for online implementation with a low complexity burden, some primary tests are needed to tune the filter parameters. Implementing an adaptive or intelligent approach to tune the filter parameters can be taken into consideration for future research.

7. REFERENCES

1. Noureldin A, Karamat TB, Georgy J. Fundamentals of inertial navigation, satellite-based positioning and their integration: Springer Science & Business Media; 2012.https://doi.org/10.1007/978-3-642-30466-8

2. El-Sheimy N, Youssef A. Inertial sensors technologies for navigation applications: State of the art and future trends. Satellite Navigation. 2020;1(1):1-21. https://doi.org/10.1186/s43020-019-0001-5

3. Farhangian F, Benzerrouk H, Landry Jr R. Opportunistic in-flight INS alignment using LEO satellites and a rotatory IMU platform. Aerospace. 2021;8(10):280. https://doi.org/10.3390/aerospace8100280

4. Ghaderi F, Toloei A, Ghasemi R. Quadrotor Control for Tracking Moving Target, and Dynamic Obstacle Avoidance Based on Potential Field Method. International Journal of Engineering, Transactions A: Basics. 2023;36(10):1720-32. https://doi.org/10.5829/IJE.2023.36.10A.01

5. Wang Q, Liu K, Cao Z. System noise variance matrix adaptive Kalman filter method for AUV INS/DVL navigation system. Ocean Engineering. 2023;267:113269. https://doi.org/10.1016/j.oceaneng.2022.113269

6. Siddharth D, Saini D, Singh P. An efficient approach for edge detection technique using kalman filter with artificial neural network. International Journal of Engineering, Transactions C: Aspects. 2021;34(12):2604-10. https://doi.org/10.5829/IJE.2021.34.12C.04

7. Valizadeh A, Hamidi H. Improvement of navigation accuracy using tightly coupled kalman filter. International Journal of Engineering, Transactions B: Applications. 2017;30(2):215-23. https://doi.org/10.5829/idosi.ije.2017.30.02b.08

8. Hooshmand M, Yaghobi H, Jazaeri M. Irradiation and Temperature Estimation with a New Extended Kalman Particle Filter for Maximum Power Point Tracking in Photovoltaic Systems. International Journal of Engineering, Transactions C: Aspects. 2023;36(6):1099-113. https://doi.org/10.5829/IJE.2023.36.06C.08

9. Morales LA, Fabara P, Pozo DF. An Intelligent Controller Based on LAMDA for Speed Control of a Three-Phase Inductor Motor. Emerging Science Journal. 2023;7(3):676-90. https://doi.org/10.28991/ESJ-2023-07-03-01

10. Bagherzadeh SZ, Toosizadeh S. Eye tracking algorithm based on multi model Kalman filter. HighTech and Innovation Journal. 2022;3(1):15-27. https://doi.org/10.28991/HIJ-2022-03-01-02

11. Wirawan IMA, Wardoyo R, Lelono D, Kusrohmaniah S. Modified Weighted Mean Filter to Improve the Baseline Reduction Approach for Emotion Recognition. Emerging Science Journal. 2022;6(6):1255-73. http://dx.doi.org/10.28991/ESJ-2022-06-06-03

12. Rahgoshay MA, Karimaghaie P. Robust in-field estimation and calibration approach for strapdown inertial navigation systems accelerometers bias acting on the vertical channel. IET Radar, Sonar & Navigation. 2020;14(3):407-14. https://doi.org/10.1049/iet-rsn.2019.0359

13. Rocha KD, Terra MH. Robust Kalman filter for systems subject to parametric uncertainties. Systems & Control Letters. 2021;157:105034. https://doi.org/10.1016/j.sysconle.2021.105034

14. Wang D, Dong Y, Li Z, Li Q, Wu J. Constrained MEMS-based GNSS/INS tightly coupled system with robust Kalman filter for accurate land vehicular navigation. IEEE Transactions on Instrumentation and Measurement. 2019;69(7):5138-48. https://doi.org /10.1109/TIM.2019.2955798

15. Zhu H, Zhang G, Li Y, Leung H. An adaptive Kalman filter with inaccurate noise covariances in the presence of outliers. IEEE Transactions on Automatic Control. 2021;67(1):374-81. https://doi.org /10.1109/TAC.2021.3056343

16. Farhangian F, Landry Jr R. Accuracy improvement of attitude determination systems using EKF-based error prediction filter and PI controller. Sensors. 2020;20(14):4055. https://doi.org/10.3390/s20144055

17. Setoodeh P, Habibi S, Haykin S. Kalman Filter. 2022. https://doi.org /10.1002/9781119078166.ch5

18. Zhang J, He X, Zhou D. Generalised proportional–integral–derivative filter. IET Control Theory & Applications. 2016;10(17):2339-47. https://doi.org/10.1049/iet-cta.2015.0610

19. Rahgoshay MA, Karimaghaie P, Shabaninia F. Robust inertial frame-based alignment of fiber-optic gyro strapdown inertial navigation systems using a generalized proportional–integral–derivative filter. Optical Engineering. 2017;56(9):095102-. https://doi.org/ 10.1117/1.OE.56.9.095102.

20. Rahgoshay MA, Karimaghaie P, Shabaninia F. Initial alignment of fiber-optic inertial navigation system with large misalignment angles based on generalized proportionalintegral-derivative filter. International Journal on Smart Sensing & Intelligent Systems. 2017;10(3). https://doi.org/10.21307/ijssis-2017-226

21. Aggarwal P. MEMS-based integrated navigation: Artech House; 2010. https://doi.org/10.1186/s43020-019-0001-5

22. Zhang W, Ghogho M, Yuan B. Mathematical model and matlab simulation of strapdown inertial navigation system. Modelling and Simulation in Engineering. 2012;2012. https://doi.org/10.1155/2012/264537

Persian Abstract

چکیده

بکارگیری یک روش موثر تلفیق داده در سیستم های ناوبری تلفیقی نقش موثری در عملکرد و دقت سیستم دارد. استفاده از یک روش موثر در تخمین نه تنها می تواند باعث بهبود دقت کلی سیستم گردد، بلکه در افزایش خاصیت مقاوم بودن سیستم در مواجه با بروز خطا و نامعینی های اندازه گیری نیز موثر خواهد بود. مساله طراحی و بکارگیری یک روش تخمین بهینه حالت و تلفیق داده که بتواند بطور همزمان دارای خاصیت مقاوم بودن و ساختار ساده برای پیاده سازی عملی باشد به یک مساله داغ در سیستم های ناوبری و موقعیت یابی بدل شده است. در این مقاله با الهام از اصول تئوری کنترل کننده های تناسبی– انتگرالی –مشتقی و ترکیب آن با تخمین گر مرسوم فیلتر کالمن، یک روش تلفیق داده مقاوم در برابر نامعینی های اندازه گیری سنسورهای کمکی در سیستم های ناوبری تلفیقی ارائه شده است. به لطف اضافه شدن ترم های انتگرالی و مشتقی به تخمین گر ساده فیلتر کالمن، سیستم ناوبری تلفیقی پیشنهادی دارای عملکرد سریع تر و دقیق تر در مقایسه با سیستم های ناوبری تلفیقی بر پایه فیلتر کالمن ساده می باشد. نتایج شبیه سازی ها نشان دهنده کارایی و برتری روش پیشنهادی نسبت به روش تلفیق مرسوم بر پایه فیلتر کالمن ساده است.